ELSEVIER

Earth and Planetary Science Letters 154 (1998) 109–125

EPSL

Sr, Nd and Pb isotopic variation along the Pacific–Antarctic risecrest, 53–57°S: Implications for the composition and dynamics of the South Pacific upper mantle

Paterno R. Castillo [a,*], James H. Natland [b], Yaoling Niu [c], Peter F. Lonsdale [a]

[a] *Scripps Institution of Oceanography, University of California, San Diego, 9500 Gilman Drive, La Jolla, CA 92093-0220, USA*
[b] *Rosenstiel School of Marine and Atmospheric Science, University of Miami, Miami, FL 33149, USA*
[c] *Department of Earth Sciences, The University of Queensland, Brisbane, Qld. 4072, Australia*

Received 22 October 1996; revised 16 September 1997; accepted 26 September 1997

Abstract

Sr, Nd and Pb isotope data for basalts from spreading axes and off-axis volcanoes near the Pacific–Antarctic risecrest, from Vacquier transform to just south of Udintsev transform, reveal an isotopically heterogeneous upper mantle. The isotopic composition of the mantle is represented by three end-members: (1) the 'depleted' source of the bulk of Pacific normal-type mid-ocean ridge basalts (N-MORB); (2) an 'enriched' source that produces basalts of the Hollister Ridge; and (3) a source, restricted to two adjacent sample locales, similar to that of Indian MORB. The distribution of these isotopic heterogeneities along the Pacific–Antarctic risecrest suggests two alternative hypotheses on the nature and dynamics of the south Pacific upper mantle. The whole area could be a single N-MORB mantle domain that shows a weak but continuous increase in $^{143}Nd/^{144}Nd$ from northeast to southwest across more than 2000 km of sea floor. The gradient is unrelated to the Louisville hotspot because Louisville basalts have low $^{143}Nd/^{144}Nd$ and the hotspot's influence along the ridge is spatially limited and near the high $^{143}Nd/^{144}Nd$ southwestern end of the gradient. The gradient appears consistent with a southwestward flow of the Pacific N-MORB-type mantle that has been proposed mainly on the basis of ridge morphology. That the N-MORB mantle domain is continuous across Heezen suggests that large-scale magmatic segmentation is not related to the largest structural offsets of the Pacific ridges. Alternatively, the higher $^{87}Sr/^{86}Sr$, ΔNd and $\Delta 8/4$ of samples from southwest of the Heezen transform relative to those from the northeast could result from southwestward pumping of both plume and Indian Ocean-type mantle material by the Louisville hotspot. The Heezen transform forms a prominent tectonic and mantle domain boundary that prohibits the Louisville- and Indian Ocean-type mantle from flowing towards and contaminating the depleted Pacific-type source in the northeast. © 1998 Elsevier Science B.V.

Keywords: Sr-87/Sr-86; Nd-144/Nd-143; Pb-208/Pb-204; isotope ratios; petrology; mid-ocean ridge basalts; Pacific-Antarctic Ridge; East Pacific Rise; South Pacific

1. Introduction

Mid-ocean ridge basalts are produced by decompression melting of mantle welling up beneath di-

* Corresponding author. Fax: +1 619 534 0784. E-mail: pcastillo@ucsd.edu

PII S0012-821X(97)00172-6

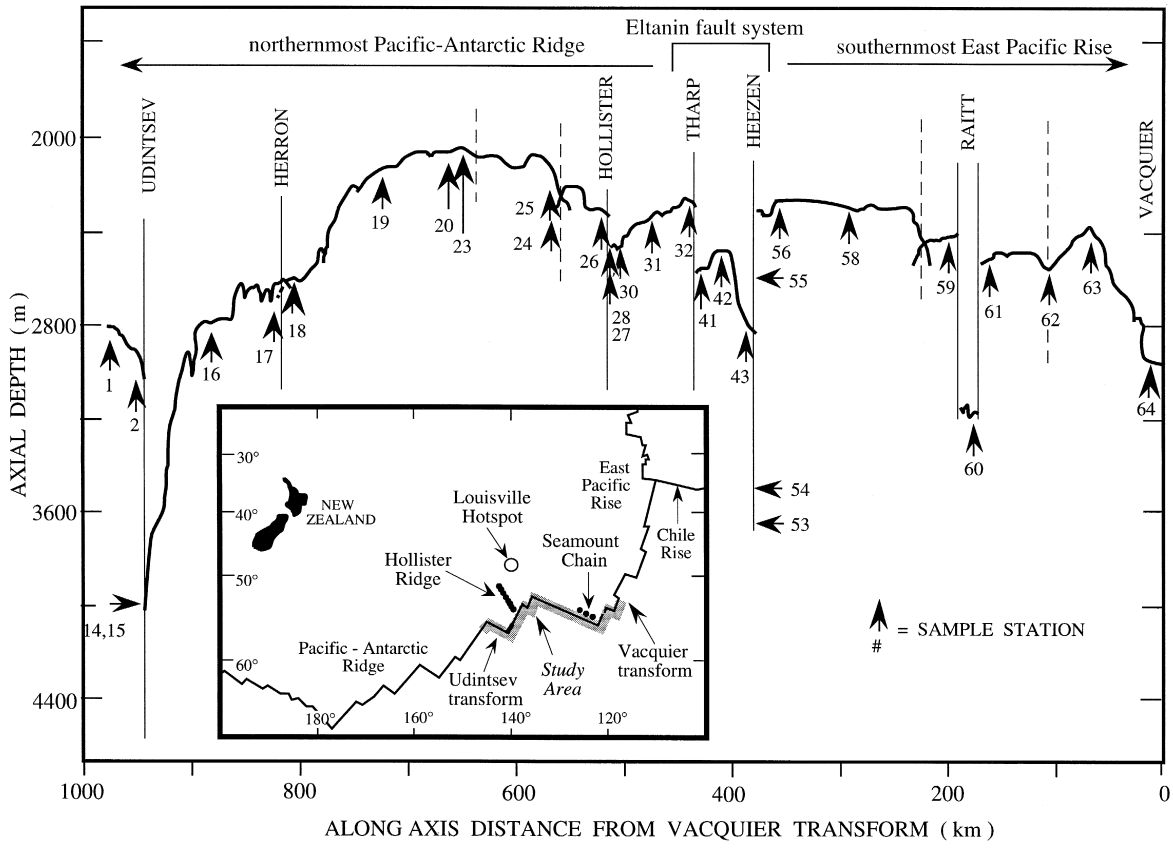

Fig. 1. Along-axis bathymetric profile of the southern EPR and northern PAR in meters below sea level, plotted versus distance from the Vacquier transform fault. Note the overall shallowing of the ridge axis from the Vacquier transform (northeast) to south of the Udintsev transform (southwest). Transform faults are indicated by solid lines, major non-transform ridge offsets by dashed lines, sampling stations by arrows and numbers. Inset shows location of the study area (shaded), bounded by the Vacquier transform in the northeast and the Udintsev transform in the southwest.

verging plate boundaries. The composition of MORB and the morphologic and geophysical characteristics of mid-ocean ridges are widely considered to be related (e.g. [1–5]). Exploration of these relationships has up until now been concentrated on the more accessible portions of the global mid-ocean ridge system in northern and tropical latitudes, particularly in the Pacific. Investigations of ridge segments at far southern latitudes are relatively few (e.g. [6–8]).

Our Seabeam mapping and rock sampling of adjoining parts of the East Pacific Rise (EPR) and Pacific–Antarctic Ridge (PAR) in the far southern Pacific during the austral summer of 1994 [9–11] represent the first systematic investigation of one of the great petrologically unknown regions of the global spreading ridge system (Fig. 1). In this paper we present Sr, Nd and Pb isotopic results on basaltic glasses obtained during our sampling. Our objectives are to constrain the composition of the MORB source along the Pacific–Antarctic risecrest, and to relate these compositions to the scale and dynamics of the upper mantle in this region of the southern Pacific.

2. Geologic setting

Our study area (Fig. 1) includes 950 km of Pacific–Antarctic spreading axis subdivided by 6 right-stepping transforms that have a combined length

of 1500 km. The two longest and most closely spaced transforms, Heezen and Tharp, are often grouped together as the Eltanin fault system; this 850 km long shear zone is one of the longest breaks in the global system of spreading centers, and is the traditional boundary between the EPR and PAR.

The crustal accretion rate along this central part of the Pacific–Antarctic plate boundary, calculated from the plate rotation model of de Mets et al. [12] and the timescale of Cande and Kent [13], decreases southward from 83 mm/yr near Vacquier transform (53°S) to 75 mm/yr near Udintsev transform (56–57°S). These are 'intermediate' spreading rates, comparable to those on the northern part of the Pacific–Cocos boundary [14] and the central Indian–Antarctic boundary [15]. As at those other intermediate-rate spreading centers, there is much variation in the structural geomorphology of the risecrest. In the faster-spreading northern half of our study area, most EPR spreading segments have axial ridges similar to those on fast-spreading risecrests but there are short axial rift valleys immediately south of the Vacquier transform (sampling station 64, Fig. 1) and within the Raitt transform (station 60) [8]. The 55 km long mid-Eltanin spreading center, between the Heezen and Tharp transforms, also has an axial ridge [16]. Along the northernmost PAR, we found, by multibeam bathymetry during our sampling cruise, that the segment immediately north of the Udintsev transform has a 1 km deep axial rift valley, the one midway between the Hollister and Herron transforms at 55°S has a 250 m high axial ridge, and most of the others have the low relief rifted morphology once thought typical of intermediate spreading rates [17]. We assume, following interpretations of other intermediate-rate spreading centers (e.g. [5,14,15]), that these structural variations result from inter-segment differences in the rate of magma supply, and that axial ridges indicate the presence of long-lived crustal magma chambers, whereas axial rift valleys indicate their absence [3].

There is a range of almost 2 km in the depth below sea-level of the spreading axis in our study area, from just over 2000 m at the summit of a broad hump in the long-profile (Fig. 1) near 55°S (station 20 and 23), to almost 4000 m in the rift valley north of the Udintsev transform (stations 14 and 15). The short, isolated intra-Raitt and mid-Eltanin axes are deeper than average. The 2035 m summit of the PAR axial ridge at 55°S is slightly shallower than any EPR axial ridge, and in the eastern Pacific is topped only by the Cocos–Nazca spreading center in the vicinity of the Galapagos hotspot [18]. The axis is shallow not because the axial ridge is unusually high, but because an axial ridge of average height rises above a broad regional shoaling of the northern PAR.

Most of our samples were collected (by chain bag dredges and wax-covered corers) from the floors of axial rift valleys, the crests of axial ridges, or the 'overshot ridge' prolongations of axial ridges around transform-fault intersections [8]. We also sampled young lavas erupted off-axis, at a chain of volcanoes and a volcanic ridge on the Pacific plate. The volcanic chain (station 57) is in the 'inside corner' between the southernmost EPR axial ridge and Heezen transform, and erupted along a fracture opened by a small component of extension across the transform [8]. Stations 21 and 22 sampled the southeastern end of the Hollister Ridge, a 1–3 km high, 450 km long volcanic ridge that extends obliquely down the western flank of the PAR, from within 10 km of the 55°S axial-ridge summit, across the Hollister fracture zone, onto ~15 Ma crust south of Tharp fracture zone. Hollister Ridge was discovered decades ago with soundings of less than 250 m by U.S.N.S. *Eltanin* [19] but its extent, shape and strike (313°) was defined more recently, by satellite altimetry (e.g. [20]). Altimetry also indicates that two or more lower ridges parallel the main ridge, 30–60 km to the southwest. We surveyed and sampled the southeast end of the Hollister Ridge, 10–75 km from the spreading axis, where it is a narrow line of coalesced volcanos. In this respect, and in overall geomorphology and setting, Hollister Ridge seems similar to many other volcanic ridges that have been described elsewhere on young, fast-moving Pacific lithosphere, notably near the Pacific–Nazca boundary at 13–19°S (e.g. [21]). Whether these ridges grow in response to regional extensional stresses in the Pacific plate [22] or to a secondary circulation in the underlying asthenosphere [23], a common feature of all explanatory hypotheses is that the ridge azimuth is parallel to the motion of the plate over the asthenosphere. For Hollister Ridge, this condition holds only if the underlying asthenosphere is moving southward in the

hotspot reference frame (see discussion below) because the ridge strikes about 17° oblique to Gripp and Gordon's [24] estimate of Pacific motion with respect to the hotspots [25]. Wessel and Kroenke [26] have suggested that this estimate of Pacific motion is quite wrong, and that for the past 3 m.y. the Pacific plate in the vicinity of Hollister Ridge has been moving (relative to the hotspots) not 296° [24], but almost due north (003°). This hypothesized Pacific motion, with a 70° change in direction at 3 Ma, places the summit of Hollister Ridge over the hotspot responsible for the Louisville seamount chain; more conventional estimates of plate motion locate this hotspot ~350 km to the northeast, near where Lonsdale [27] surveyed and sampled a large Pleistocene seamount with distinctively Louisville geochemistry [28]. We reject Wessel and Kroenke's [26] 'relocation' of the hotspot on tectonic grounds because the geography of the Pacific–Antarctic risecrest is inconsistent with their hypothetical Pacific motion (there is no evidence of such a radical realignment of spreading axes and transforms at 3 Ma), and the geomorphology and pattern of Hollister ridge and its partners are quite unlike typical manifestations of the Louisville (or any other) hotspot. A more relevant question, which we will address below, is whether a Louisville hotspot located hundreds of kilometers to the north beneath the EPR flank [27] could increase the mantle temperature and magma supply of the northern PAR, and thereby explain its shallow depth and the prolific volcanism evidenced by an axial ridge along the spreading center and high ridges along rise-flank fractures.

3. Samples and methodology

Samples from the ridge axes, overshot ridges and intratransform centers include both primitive and moderately differentiated tholeiitic basalts, a ferroandesite and a dacite. Off-axis samples include tholeiitic basalts and a few mildly alkalic basalts from Hollister Ridge [10–12]. An important feature of Pacific–Antarctic risecrest basalts is their overall similarity in their chemical composition with those from the better sampled intermediate- to fast-spreading sections of the EPR north of ~30°S, henceforth referred to as the 'northerly EPR'. Consistent with previous studies (e.g. [29,30]), we have chosen to subdivide our basalt samples into geochemical groups using K/Ti ratio. Basalts from the Pacific–Antarctic risecrest, similar to those from the northerly EPR, are dominated by depleted, low K/Ti (<0.14) N-MORB. There are a few transitional-type (T-)MORB ($K/Ti > 0.14$) along the Pacific–Antarctic risecrest although these are fairly common in the northerly EPR (e.g. [1,29,30]). In the Pacific–Antarctic risecrest, T-MORB grade compositionally into enriched ($K/Ti > 0.56$), mildly alkalic basalts from the southeastern end of Hollister Ridge. Some near-ridge seamounts along the northerly EPR are also capped with alkalic basalts (e.g. [31]). Finally, a few compositionally distinct, highly primitive and extremely depleted basalts were collected from the Raitt intratransform spreading center. These samples are chemically similar to those from the Garret and Siquieros intratransform domains [32–34].

Samples analyzed for Sr, Nd and Pb isotopic

Note to Table 1:

All Sr and Nd isotope analyses were done at the Scripps Institution of Oceanography; all Pb isotope analyses were made at the San Diego State University (Dr. B. Hanan, analyst). ± values are in-run precisions and refer to the last digits of the isotopic ratios. Multiple determinations of NBS 987 ($^{87}Sr/^{86}Sr = 0.71025$) give analytical uncertainty of ± 0.000020 for $^{87}Sr/^{86}Sr$; multiple determinations of the La Jolla Nd standard ($^{143}Nd/^{144}Nd = 0.511860$) give analytical uncertainty of ± 0.000016 for $^{143}Nd/^{144}Nd$; analytical uncertainties on Pb isotopic ratios, based on error propagation of the error in NBS 981 values and the analytical precision errors in the sample determination, are approximately ± 0.005 for $^{206}Pb/^{204}Pb$ and $^{207}Pb/^{204}Pb$ and ± 0.01 for $^{208}Pb/^{204}Pb$. Sr isotopic ratios were fractionation-corrected to $^{86}Sr/^{88}Sr = 0.1194$; Nd isotopic ratios were measured in oxide forms and fractionation corrected to $^{146}NdO/^{144}NdO = 00.72225$ ($^{146}Nd/^{144}Nd = 0.7219$); Pb isotopic ratios were corrected for mass fractionation based on average measured values for NBS 981 using the values of Todt et al. [54]. Sample preparation was done at Scripps. Total procedural blanks are <20 pg for Sr and <5 pg for Nd (~30 mg samples) and <0.5 ng for Pb (300–400 mg samples). Trace element data acquired through ICP–MS at Scripps using the procedure described in Janney and Castillo [35]. Reproducibility for the method is generally better than 4% based on repeated analyses of international standards AGV-1 and BCR-1 and of an in-house standard of an EPR basalt. La/Sm(chon) = chondrite-normalized [52] La/Sm values. Major element data acquired through electron probe at the University of Queensland. TiO_2 and Na_2O fractionation-corrected values are for major element contents corrected for fractionation to 8 wt% MgO using the method described in Niu and Batiza [2].

Table 1
Sr, Nd and Pb isotopic ratios, incompatible element ratios and fractionation-corrected major element composition of representative south Pacific basalts

Sample	Lat. (South)	Long. (West)	$^{87}Sr/^{86}Sr$	(±)	$^{143}Nd/^{144}Nd$	(±)	$^{206}Pb/^{204}Pb$	(±)	$^{207}Pb/^{204}Pb$	(±)	$^{208}Pb/^{204}Pb$	(±)	K/Ti	Ba/Ti (*100)	La/Sm (chon)	Ti_8	Na_8
Normal-MORB																	
D1-2	55.90	144.91	0.702502	19	0.513113	9							0.117	0.18	0.73	1.28	2.60
D7-7-1	56.02	143.87	0.702536	14	0.513158	8							0.108	0.14	0.71	1.17	2.78
D14-1	56.11	140.17	0.702442	18	0.513173	11	18.203	0.001	15.448	0.001	37.618	0.002	0.059	0.09	0.48	1.33	2.56
D16-7A	56.68	139.67	0.702433	18	0.513199	8	17.981	0.001	15.445	0.001	37.363	0.003	0.067	0.08	0.49	1.27	2.87
D17-2A	56.27	139.31	0.702423	14	0.513177	9	18.297	0.004	15.484	0.003	37.815	0.008	0.054	0.05	0.45	1.33	2.58
D18-1	56.25	138.88	0.702678	10	0.513076	9	18.732	0.002	15.501	0.001	38.184	0.003	0.080	0.16	0.79	1.65	2.63
GC32	53.92	134.57	0.702787	14	0.513152	7	17.684	0.008	15.460	0.007	37.216	0.016	0.120	0.40	0.65	1.17	2.46
D41-2	55.33	127.76	0.702352	16	0.513174	7							0.074	0.08	0.58	1.36	2.87
D42-1A	55.10	127.61	0.702336	16	0.513165	7	18.039	0.002	15.433	0.002	37.363	0.005	0.076	0.07	0.56	1.33	2.87
D53-1B	55.76	122.89	0.702487	17	0.513103	10	18.444	0.004	15.493	0.003	37.761	0.008	0.119	0.15	0.78	1.46	2.69
D56-1	55.67	121.44	0.702512	11	0.513109	9							0.101	0.13	0.75	1.32	2.75
D58-1	55.15	121.14	0.702524	16	0.513090	10							0.112	0.15	0.85	1.48	2.77
D60-1A	54.43	119.35	0.702945	22	0.512991	9	18.497	0.002	15.560	0.002	37.838	0.004	0.052	0.03	0.35	1.53	2.97
D60-2	54.43	119.35	0.702954	20	0.512987	6	18.508	0.001	15.542	0.001	37.764	0.002	0.054	0.03	0.33	1.52	2.92
D61-1	54.45	118.42	0.702452	21	0.513090	9							0.090	0.08	0.71	1.36	2.73
D62-1A	54.01	118.14	0.702441	14	0.513111	8							0.088	0.15	0.74	1.56	2.74
D63-1A	53.67	117.97	0.702540	14	0.513065	9	18.882	0.002	15.538	0.001	38.194	0.003	0.110	0.27	0.89	1.47	2.73
D64-2	53.13	117.70	0.702415	23	0.513090	8	18.805	0.003	15.506	0.003	38.075	0.007	0.057	0.10	0.62	1.60	2.35
D64-3B	53.13	117.70	0.702418	13	0.513106	7							0.057	0.10	0.62	1.79	2.38
Transitional-MORB																	
D31-1B	54.27	134.89	0.702852	20	0.513163	12	17.852	0.002	15.441	0.001	37.303	0.003	0.154	0.38	0.75	1.21	2.63
D23-1	54.88	137.67	0.702824	24	0.513060	9							0.142	0.31	0.89	1.25	2.65
D23-3E	54.88	137.67	0.703508	14	0.512978	7	18.768	0.002	15.536	0.001	38.377	0.003	0.210	0.53	1.37	1.67	2.84
D59-1	54.31	120.77	0.702417	12	0.513122	9							0.175	0.19	0.95	1.26	2.74
Seamounts / Hollister Ridge																	
D21-2B	54.59	138.53	0.702624	14	0.513113	8							0.061	0.08	0.55	1.70	2.89
D21-6E	54.59	138.53	0.703486	22	0.512922	8	18.889	0.002	15.539	0.002	38.665	0.004	0.574	1.14	2.34	1.99	3.55
D22-1A	54.84	137.88	0.703518	22	0.512974	9	18.782	0.010	15.544	0.008	38.397	0.021	0.273	0.54	1.40	1.62	2.84
D57-3	55.56	122.17	0.702536	14	0.513067	10	18.498	0.005	15.518	0.004	37.749	0.009	0.162	0.24	0.88	1.46	2.75

ratios were first ground into 1–2 cm sized fragments in a stainless steel mortar and pestle, and then sonically cleaned in distilled water. After drying, glass fragments free of phenocrysts and alterations were hand picked under a binocular microscope. The selected glass fragments were sonically cleaned again in distilled water and then acetone. Finally, glass samples for isotopic analysis were leached with warm, ~2.0 N HCl for about 15 min prior to dissolution. Isotopic analyses and some trace element data of selected glass samples from the study area are presented in Table 1. Analytical procedures for isotopic analysis are listed as notes in Table 1; analytical procedures for major and trace element analysis are presented elsewhere ([35]; manuscript in prep.).

4. Analytical results

The Pacific–Antarctic lavas are isotopically heterogeneous, but their Sr, Nd and Pb isotopic ratios display overall correspondence and their

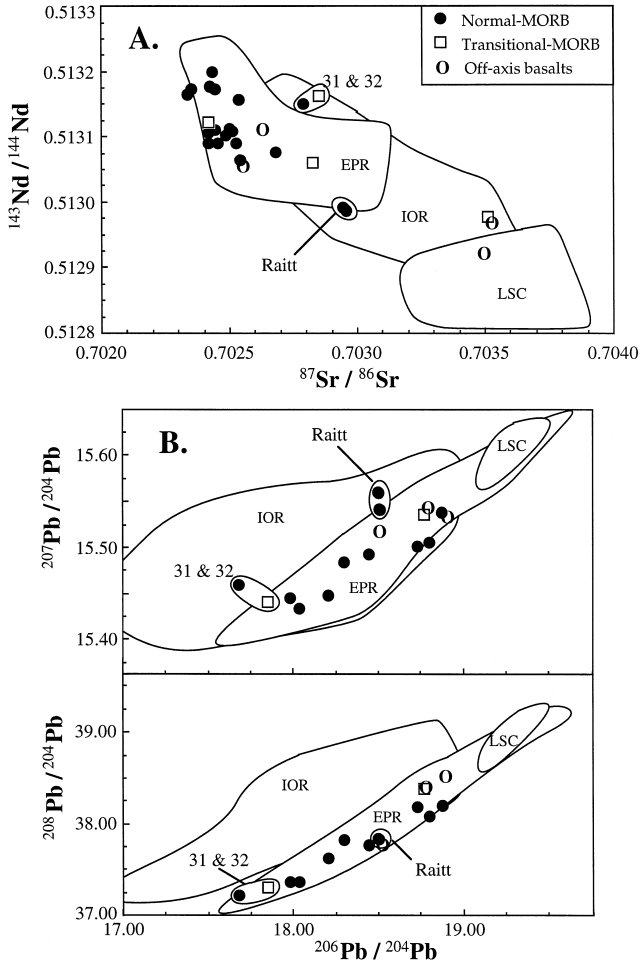

Fig. 2. (A) $^{87}Sr/^{86}Sr$ versus $^{143}Nd/^{144}Nd$ and (B) $^{206}Pb/^{204}Pb$ versus $^{207}Pb/^{204}Pb$ and $^{208}Pb/^{204}Pb$ ratios for the Pacific–Antarctic basalts listed in Table 1. Typical analytical uncertainties are about the size or smaller than the symbols used. Fields for MORB from the Indian Ocean ridges (IOR), East Pacific Rise (EPR) and Louisville Seamount Chain (LSC) are shown for reference. Sources of data are from [6,7,28,37–43] and references therein. Data for samples D31-1B (T-MORB), GC32 (N-MORB) and N-MORB from the Raitt intratransform spreading center are labelled separately for clarity. Off-axis samples represent samples from the linear volcanic chain in the inside corner of Heezen and from the southeastern end of Hollister Ridge.

$^{206}Pb/^{204}Pb$ ratios correlate well with $^{207}Pb/^{204}Pb$ and $^{208}Pb/^{204}Pb$ (Figs. 2 and 3). Pacific–Antarctic N-MORB are similar to typical ridge basalts elsewhere, being depleted in incompatible trace elements and having variable but generally low $^{87}Sr/^{86}Sr$ and high $^{143}Nd/^{144}Nd$ ratios, except for those from the Raitt intratransform spreading center (Fig. 2A). The intratransform basalts have relatively higher $^{87}Sr/^{86}Sr$ and lower $^{143}Nd/^{144}Nd$ than the other N-MORB, despite their extreme depletion in incompatible elements; they plot at the high $^{87}Sr/^{86}Sr$ and low $^{143}Nd/^{144}Nd$ end of the MORB field for the northerly EPR, approaching the composition of the Louisville Seamount Chain lavas. Moreover, samples GC32 and D31-1B, which are N-MORB and T-MORB, respectively, from a short PAR segment bounded by the Hollister and Tharp transforms, have slightly higher $^{87}Sr/^{86}Sr$ for given $^{143}Nd/^{144}Nd$ than the other Pacific–Antarctic N-MORB and the EPR MORB. The Sr and Nd isotopic ratios of Pacific–Antarctic T-MORB are variable, ranging from low $^{87}Sr/^{86}Sr$ and high $^{143}Nd/^{144}Nd$, similar to the majority of the N-MORB, to high $^{87}Sr/^{86}Sr$ and low $^{143}Nd/^{144}Nd$, close to those of the Louisville Seamount Chain lavas. The sample from the volcanic chain in the inside corner of Heezen transform has low $^{87}Sr/^{86}Sr$ but high $^{143}Nd/^{144}Nd$ similar to the N-MORB, but samples from Hollister Ridge have Sr and Nd isotopic values that overlap with those of the Louisville Seamount Chain lavas. The Pb isotope ratios (Fig. 2B) of all Pacific–Antarctic ridge basalts overlap and generally fall within the EPR MORB field in the $^{206}Pb/^{204}Pb$ versus $^{208}Pb/^{204}Pb$ diagram. However, the intratransform N-MORB and samples D31-1B and GC32 have relatively higher $^{207}Pb/^{204}Pb$ for given $^{206}Pb/^{204}Pb$ than the rest of the ridge basalts (Fig. 2B). Samples from the Hollister Ridge have among the highest $^{206}Pb/^{204}Pb$ and plot close to, although do not overlap, values of the Louisville Seamount Chain lavas.

Additional details of the isotopic characteristics of the Pacific–Antarctic lavas are shown by the plots of $^{87}Sr/^{86}Sr$ and $^{143}Nd/^{144}Nd$ versus $^{206}Pb/^{204}Pb$ (Fig. 3A,B). The majority of Pacific–Antarctic N-MORB data indeed plot inside the EPR MORB field; data for the volcanic chain in the inside corner of Heezen transform also plot within the EPR MORB field. Samples GC32 and D31-1B plot outside the

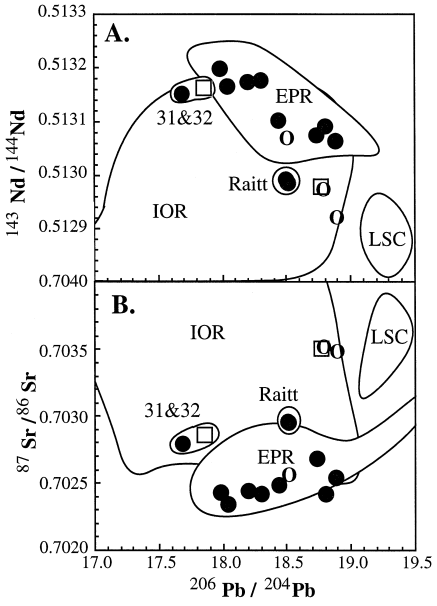

Fig. 3. $^{206}Pb/^{204}Pb$ versus (A) $^{87}Sr/^{86}Sr$ and (B) $^{143}Nd/^{144}Nd$ ratios for Pacific–Antarctic basalts. Symbols and sources of data as in Fig. 2.

EPR field, but within the field for MORB from the Indian Ocean ridges. Raitt intratransform and off-axis basalt data also plot outside the EPR field, and inside the field for MORB from the Indian Ocean ridges. Hollister Ridge basalts do not plot inside the Louisville Seamount Chain field because they have low $^{206}Pb/^{204}Pb$ for given $^{87}Sr/^{86}Sr$ and $^{143}Nd/^{144}Nd$ relative to the Louisville Seamount Chain lavas. They are isotopically similar to the lavas from seamounts in the central and northern portions of the Hollister Ridge ([36]; L. Dosso, pers. commun., 1997). Thus, lavas from Hollister Ridge may not have entirely originated from the Louisville mantle plume, but from a mixture of Louisville and depleted EPR mantle materials.

Except for the Raitt intratransform basalts and samples GC32 and D31-1B, the $^{87}Sr/^{86}Sr$, $^{143}Nd/^{144}Nd$ and $^{207}Pb/^{204}Pb$ of Pacific–Antarctic ridge and off-axis basalts show good correlations with highly/moderately incompatible element ratios, from the most depleted abyssal tholeiites to the Hollister alkalic basalt (correlation coefficients, r, are > 0.80; Fig. 4A–F). Correlations of $^{206}Pb/^{204}Pb$ and $^{208}Pb/^{204}$ with the majority of highly/moderately incompatible element ratios for the Pacific–

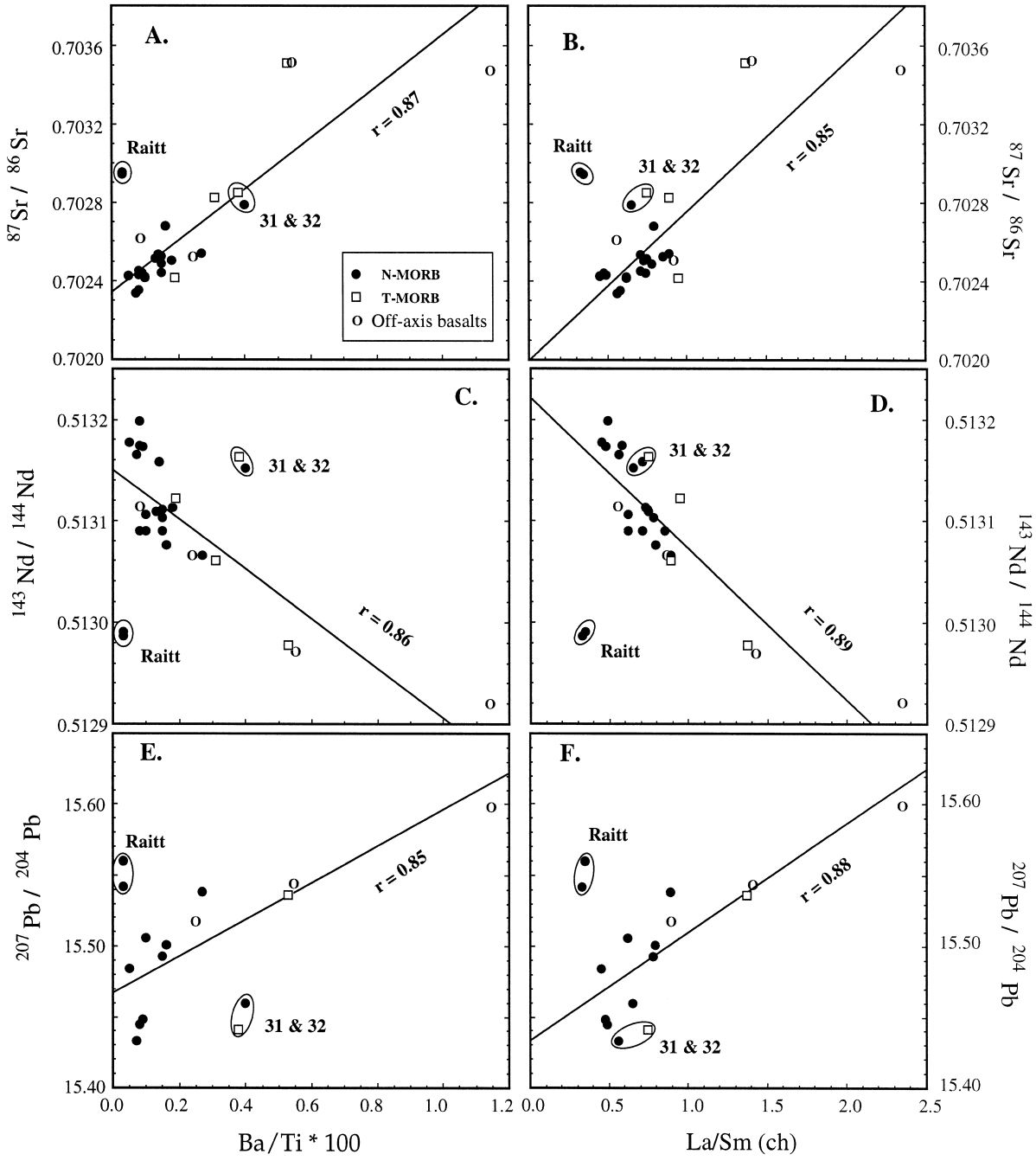

Fig. 4. (A)–(F) $^{87}Sr/^{86}Sr$, $^{143}Nd/^{144}Nd$ and $^{207}Pb/^{204}Pb$ versus Ba/Ti and chondrite-normalized La/Sm ratios for Pacific–Antarctic basalts. Chondrite normalizing values are from [55]. Correlation coefficients (r values) for the regression lines are calculated for all the basalts except for the Raitt intratransform, D31-1B and GC32 basalts. Plots of $^{87}Sr/^{86}Sr$ and $^{143}Nd/^{144}Nd$ versus other highly/moderately incompatible element ratios such as Rb/Ti, K/Ti, K/P and Sm/Nd also yield similarly high correlation coefficient values ($r > 0.80$).

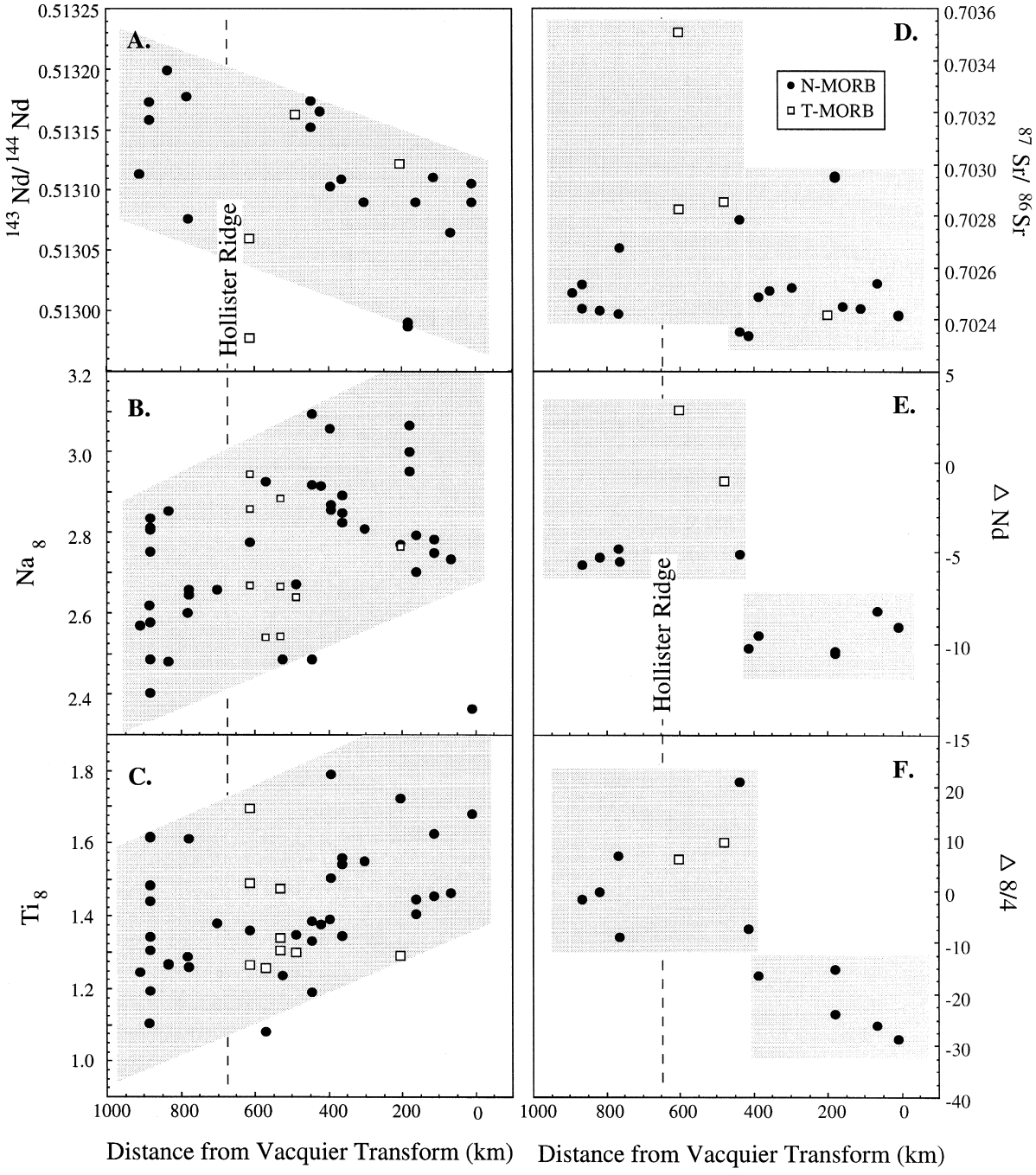

Fig. 5. Variations of (A) $^{143}Nd/^{144}Nd$; (B) Na_8; (C) Ti_8; (D) $^{87}Sr/^{86}Sr$; (E) ΔNd; and (F) $\Delta 8/4$ of MORB vs. distance from Vacquier transform along the Pacific–Antarctic risecrest. Data are interpreted as either a weak overall increase in $^{143}Nd/^{144}Nd$ and decreases in Na_8 and Ti_8 of N-MORB from the northeast (Vacquier transform) toward the southwest (Udintsev transform) (A)–(C) or a systematically higher $^{87}Sr/^{86}Sr$, ΔNd, and $\Delta 8/4$ of the northern PAR (southwest of Heezen transform) relative to the southern EPR (northeast of Heezen) (D)–(F). The approximate location of the intersection of the PAR with Hollister Ridge, which has low $^{143}Nd/^{144}Nd$ and high Na_8, Ti_8, $^{87}Sr/^{86}Sr$, ΔNd, and $\Delta 8/4$, is shown for reference. Off-axis basalt data are not shown for clarity.

Antarctic basalts also generally exist but are not as good as those with $^{87}Sr/^{86}Sr$, $^{143}Nd/^{144}Nd$ and $^{207}Pb/^{204}Pb$ ($r < 0.65$), except that $^{206}Pb/^{204}Pb$ is well correlated with Rb/Sr ($r = 0.78$, not shown). Although the good correlations are mainly controlled by the few extreme values of T-MORB and enriched Hollister Ridge basalts, similar though more limited trends are generally shown by the N-MORB alone. Thus, our data suggest that the Sr, Nd and Pb isotopic and incompatible element ratios are generally coupled in the majority of Pacific–Antarctic basalts. This observation contrasts with that in the superfast spreading southern EPR at 13–23°S where the Nd, Sr and Pb isotopic ratios of MORB are totally decoupled from trace element ratios [37,38]. Sr, Nd and Pb isotopic and incompatible element ratios are decoupled only in a few samples such as samples D31-1B and GC32 and the Raitt intratransform basalts. The intratransform basalts have somewhat higher $^{87}Sr/^{86}Sr$ and lower $^{143}Nd/^{144}Nd$ than they might, given their extremely low concentrations of highly incompatible elements. An Indian MORB-type mantle, proportionally higher in $^{87}Sr/^{86}Sr$ and Ba/Ti than other N-MORB (Table 1 and Fig. 4), is represented by samples GC32 and D31-1B from the two adjacent sampling stations, 31 and 32, in the PAR segment between the Hollister and Tharp transforms (Fig. 1).

Finally, N-MORB northeast of the Udintsev transform have higher $^{143}Nd/^{144}Nd$ than those from the EPR southwest of the Vacquier transform. The difference reflects a weak, gradual increase in $^{143}Nd/^{144}Nd$ to the southwest, from the Vacquier to Udintsev transform (Fig. 5A). Note that the Raitt intratransform basalts appear to control the low end of the gradient but, even if these are excluded from the N-MORB group, the rest of the samples still show a general increase in the range of $^{143}Nd/^{144}Nd$ to the southwest. Sr isotopic ratios show only a slight overall decrease in the range of $^{87}Sr/^{86}Sr$ toward the same direction (Fig. 5D) but a clear systematic decrease in $^{87}Sr/^{86}Sr$ to the southwest is observed along the PAR immediately west of our study area, from the Udintsev transform to 63°27′S, 166°04°W [36]. Slight along-axis decreases from northeast to southwest in Na_2O and TiO_2 contents corrected for fractionation to 8 wt% MgO (Na_8 and Ti_8, respectively; Fig. 5B,C) of the different sample groups of Pacific–Antarctic N-MORB also exist. In contrast to $^{143}Nd/^{144}Nd$ values, which represent individual samples, the Na_8 and Ti_8 values represent averages of compositionally identical (within analytical error) samples from a given sampling station. These geographical patterns of the Ti_8 and Na_8 signify an orderly spatial variation in the bulk major element composition of the upper mantle beneath the Pacific–Antarctic risecrest.

Another way of looking at the data is to consider a stepped rather than a gradational transition in isotopes along these ridges, with the step corresponding to the long offset across the two transform faults of the Eltanin system. The two geographical groups are shown by plots of $^{87}Sr/^{86}Sr$, ΔNd and $\Delta 8/4$ values versus along axis distance (Fig. 5D–F). ΔNd represents deviations of $^{143}Nd/^{144}Nd$ from the mantle plane and $\Delta 8/4$ represents departures of $^{208}Pb/^{204}Pb$ from the northern hemisphere reference line [39,40]. The peak in all of these values is centered on the geographic intersection of the Hollister Ridge with the PAR, suggesting that the Louisville hotspot influences the isotopic signature of a fairly broad region of the mantle underlying the Pacific–Antarctic risecrest.

5. Discussion

The variable isotopic and highly/moderately incompatible element ratios of Pacific–Antarctic risecrest and off-axis basalts indicate that the upper mantle there, like that beneath the northerly EPR and northeast Pacific ridges, is compositionally heterogeneous (e.g. [37,38,41–43]). The overall pattern of these heterogeneities among Pacific–Antarctic N-MORB (Fig. 5A–F) leads us to propose two alternative hypotheses about dynamic processes in the mantle beneath the Pacific–Antarctic risecrest.

5.1. A southwestward flow of the South Pacific upper mantle

This hypothesis is based on the premise that, although the gradients in $^{143}Nd/^{144}Nd$ and Na_8 and Ti_8 values among N-MORB in our study area are weak, these nevertheless represent a coherent geochemical structure of the N-MORB mantle source in the South Pacific. The large geochemical anomaly at

the PAR–Hollister Ridge intersection caused by the influence of the Louisville plume is neither related to, nor responsible for, the geochemical gradient among N-MORB. First, Hollister Ridge lavas (this study; [36]) and Louisville seamount chain lavas [28] have low $^{143}Nd/^{144}Nd$ and are enriched in incompatible elements; these are unlike the high $^{143}Nd/^{144}Nd$ and incompatible element depleted N-MORB just north of Udintsev (Fig. 4A–C). Second, the occurrence along the Pacific–Antarctic risecrest of plume-influenced T-MORB is merely as co-incidental as the occurrence of transitional-MORB and enriched-MORB on some ridge axes near other non-hotspot seamount provinces (e.g. [31,44]). Hollister Ridge, itself, thus is not necessarily related tectonically to the Louisville Seamount Chain, as summarized earlier from the perspective of its location and orientation, although the isotopic similarity between the Hollister and Louisville lavas suggests that the ridge and seamounts share a common source. The question then is: what is the cause of the southwestward gradation in composition among N-MORB?

Several morphologic and geochemical studies of southern Pacific ridges [7,45–48] have proposed that the Pacific upper mantle is flowing southwestward. We suggest that this could be responsible for the observed geochemical gradient in our region. Based on the composition of MORB from the PAR and Southeast Indian Ridge on the east and west sides of the Australian–Antarctic Discordance (AAD), respectively, Pyle et al. ([7]; see also [45]) have proposed that Pacific asthenosphere has been flowing southwestward during the last 30 m.y., displacing the Indian Ocean upper mantle between Australia and Antarctica. Such flow may have resulted from shrinkage of the Pacific region as the Gondwanan plates grew [46]. More recent interpretations suggest that evidence for the southwestward flow of the Pacific asthenosphere also occurs along the PAR between the AAD and Udintsev transform [47,48]. This includes: (1) the occurrence of abrupt changes in ridge morphology and subsidence of the ridge, from rift valley with small subsidence to axial high with normal subsidence, across Fracture Zone XII at ~64°S, 171°W [47]; and (2) the presence of a boundary between rough and faulted seafloor and smooth seafloor in the segment between the Udintsev transform and 157°W [48]. Although these are ridge-axis morphological features, the fact that there is a systematic decrease in $^{87}Sr/^{86}Sr$ along the PAR from the Udintsev transform to 63°27′S, 166°04′W [36], which is part of the proposed area of mantle flow, indicates that there may indeed be a relationship between morphologic expression of the spreading axis and the composition of the upper mantle. Thus, we envision that pulses or waves of high $^{143}Nd/^{144}Nd$ Pacific N-MORB mantle come from northeast of the Vacquier transform and flow toward the AAD.

Under this hypothesis, an Indian MORB-type mantle, like the Louisville mantle plume, is simply entrained into a large southwestward flow of depleted Pacific-type asthenosphere. However, the exact origin of the Indian MORB-type source is unknown. This could have been simply swept upward by the Louisville mantle plume, but the presence of Indian MORB-like lavas along the Chile Rise farther to the east [49] indicates that it is not a unique feature of the Louisville hotspot. Perhaps, designation of 'Indian MORB-type' mantle implies no genetic link with the Indian Ocean; therefore, similar mantle at remote locations elsewhere reflects a process that may be or have been dominant in the Indian Ocean, but is not restricted to it. For example, the Indian Ocean-like mantle material could have originated all the way from the south Central Pacific, where the large concentration of hotspots suggests a large-mantle convection, sweeping up lower mantle materials [40,50]. Alternatively, the process usually invoked for the Indian Ocean mantle is that of involvement or retention of regions, or even streaks, of subcontinental mantle left from the dispersal of Gondwanan continents and continental fragments in the widening ocean basins (e.g. [6]). The Eltanin fault system can be traced toward Antarctica to the southeast and toward the general area of the Chatham Rise, which is a continental fragment, to the northwest. These continental boundaries allow us to speculate that small fragments of old subcontinental mantle may be dispersed as far away as the modern Pacific–Antarctic risecrest in the Eltanin region. In either process, the production of Indian Ocean-type mantle has little to do with the Indian Ocean. Still another possibility is that these lavas could result from interaction of mantle melt with hydrothermally altered oceanic crust, rich in hydrothermally mobile

components such as ^{87}Sr and Ba, although the characteristically low $^{206}Pb/^{204}Pb$ of these lavas make this possibility unlikely. We thus see that Indian MORB-type mantle in this region could have come from sources other than the Louisville plume. The distinctive Pb and Sr isotopic signature and high Ba content of the basalts suggest that their mantle source is different from those of the Hollister lavas and Pacific–Antarctic N-MORB (Figs. 2–4 and Figs. 6).

As mentioned earlier, this asthenospheric flow may also be responsible for the azimuth of Hollister Ridge and the other ridges parallel to it, which could be the vector sum of the northwestward and southwestward motions of the Pacific plate and asthenosphere, respectively. The Hollister family of ridges are a plate-tectonic feature of yet unknown origin (cf. [22,23,25]). Hollister Ridge is the largest and most prominent among these ridges because it is the northernmost and longest, so that it was able to tap most of the Louisville plume material entrained in the southwest-flowing asthenosphere. Louisville plume material has been ascending near the Pacific–Antarctic risecrest and Eltanin fault system for more than 40 million years [27,28] and this material consequently displaces and eventually joins surrounding masses of depleted MORB asthenosphere flowing to the southwest. Thus the isotopic composition of Hollister Ridge connects the Louisville plume with the Pacific–Antarctic N-MORB source (Fig. 6). In addition to giving Hollister Ridge its distinctive isotopic signature, the Louisville plume also enhances production of crust and greater total volume of melting along both Hollister Ridge and its intersection with the PAR because the plume mainly consists of enriched, low temperature melting peridotites.

The asthenospheric flow proposed in this hypothesis is not restricted to this region because it also evidently occurs, albeit in a more subtle form, along the superfast spreading segment of the EPR at 13–23°S. There, highly/moderately incompatible element ratios consistently decrease from north to south along the entire segment but Sr, Nd and Pb isotopic ratios define a broad, smooth peak between 15°48′S and 20°52′S, with a maximum enrichment at 17–17°30′S [37,38]. Mahoney et al. [38] proposed that the material with plume-like isotopic composition that causes this isotopic hump may have originated

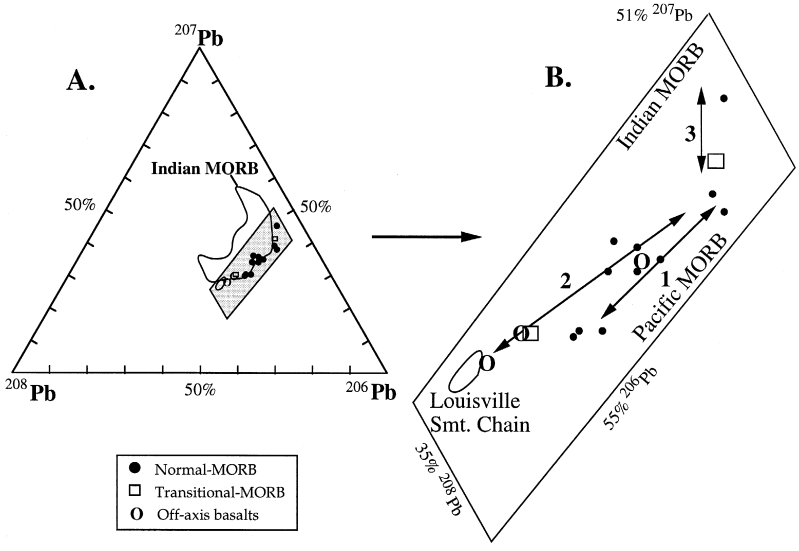

Fig. 6. (A) Triangular plot of relative abundance of ^{207}Pb, ^{208}Pb and ^{206}Pb in Pacific–Antarctic basalts. The compositional ranges of ^{207}Pb, ^{208}Pb and ^{206}Pb in the whole triangle are 15.00–16.00, 37.00–40.00 and 16.50–20, respectively. Also plotted in the triangle is the field for Indian MORB Pb isotopes for reference (from [6,41] and references therein). (B) Enlarged view of the shaded portion in the triangle. The 3 lines with arrows represent the three isotopic groups mentioned in the text: *1* = Pacific N-MORB array, *2* = Louisville plume and depleted Pacific–Antarctic MORB mixing trend, and *3* = depleted Pacific–Antarctic MORB and Indian MORB, specifically the low ^{206}Pb and high ^{207}Pb type, mixing trend.

long ago from a distant hotspot which now lies embedded in the MORB mantle matrix. One of the possible sources of the material is the Marquesas hotspot in the south Central Pacific, separated from the East Pacific risecrest with lithosphere riddled with subparallel volcanic ridges, in many ways similar to the Hollister ridges on the north flank of the PAR. Thus, in both the Pacific–Antarctic South Pacific and southern Equatorial Pacific, the Pacific plate moves over an asthenosphere that appears to move in different directions; in the former, the asthenosphere is moving toward the southwest and in the latter it seems to be moving toward the east. The origin and exact direction of movement of the asthenosphere are beyond the scope of our study but may be related to the yet unknown component of plate tectonic motion — that of the internal structure of mantle convection, which is decoupled from observable lithospheric motions.

5.2. Pacific–Antarctic Ridge–Louisville hotspot interaction

Our second hypothesis is based on the geochemical anomaly centered on the intersection of the PAR with Hollister Ridge. Here the PAR is also shallowest, it has an inflated axial cross section, and it has a correspondingly pronounced positive axial gravity anomaly [20]. These isotopic and geographic perturbations are commonly observed along the mid-ocean ridge when a hotspot is close to the risecrest (e.g. [18,43,51]). In our model, lateral mantle flow at the base of the lithosphere will be guided southward by the step-wise thinner lithosphere beneath the Eltanin system. Because of the right-lateral offsets on the fracture zones, the lithosphere is thinner to the south of the Louisville hotspot (Fig. 1); this is the direction of pressure release for lateral flow in the shallow asthenosphere. Another possibility is that Hollister Ridge is a natural consequence of a spreading center migrating toward a hotspot. Small [25] proposed that, in such a case, plume material is redistributed and migrates updip along the base of the lithosphere, away from the cool end of the spreading center toward the hotter and thinner center of the segment. In this scenario, Hollister Ridge is the trace of Louisville plume material migrating from its colder, northerly location toward PAR segments south of the Eltanin fault system.

The simplest case, of course, would be if the Louisville hotspot is located along Hollister Ridge [26]. We have ruled out this possibility earlier but, even if this is the situation, the stepped increases in thicknesses of the lithosphere across the Eltanin fault system block the lateral asthenospheric flow at the base of the lithosphere to the east and north. The result is accumulation of upwelling mantle beneath, and a responsive southward flow along, the nearest adjacent ridge axis. The most immediate effect on ridge elevation is along the nearest adjacent segment.

Thus, no matter where the hotspot is, some southward flow of shallow asthenosphere along or adjacent to the ridge axis, and pushed by the Louisville plume, is predicted. Besides the shallow, inflated ridges, such flow might also produce deviatoric stresses on the base of the thin lithosphere, which would account for the obliquity of Hollister Ridge to any plausible hotspot trace, as well as to the axis of the Pacific–Antarctic risecrest. As in the previous hypothesis, diverted flow also provides a mechanism explaining the plume-like geochemical signature of basalts from Hollister Ridge. Whatever Hollister Ridge is structurally, with its unusual orientation, and in relationship to the hotspot, it appears to be a particularly close encroachment of the plume-induced high-pressure region on the adjacent spreading centers, which accentuates both subaxial mantle flow and ridge topography. Neither elevation nor inflation of risecrest topography require that the Louisville plume impinge directly on the spreading center but they are a result of its proximity. Hence, the Hollister Ridge, and the other ridges concentric to it on the Pacific ridge flank, are consequences of volcanism along oblique rents in the sea floor caused by southwestward lateral pumping of asthenosphere along the ridge axis, prompted by proximity to the Louisville plume.

The pumping of the Louisville plume material southwest to the PAR is responsible for the step-wise increase in $^{87}Sr/^{86}Sr$, ΔNd and $\Delta 8/4$ values in the northern PAR (Fig. 4C–E). The Hollister Ridge alkalic basalt falls within, or close to, the plotted field for the Louisville Seamount Chain, the enriched potential mixing end-member in all permutations of the Sr, Nd and Pb isotope diagrams (Figs. 2 and 3).

Together, Louisville and Hollister form a linear data array that trends to the low $^{206}Pb/^{204}Pb$ end of the Pacific–Antarctic N-MORB array (Fig. 6). All points are a strong indication that the trends result from simple two-component mixing, with one end-member being represented by the most depleted abyssal tholeiite in the region, the other by the alkalic basalt from Louisville hotspot. The mixing may occur at crustal levels, between magma batches, or by blending of melt strains near the mantle source (e.g. [42]): it does not matter which. That the mantle itself is sharply partitioned into strongly depleted and more enriched zones on a very small scale is indicated by the occurrence of samples near both extremes even in single dredge hauls (cf. [32]). The enriched components within the mantle are dominated by the one end-member represented by Hollister Ridge alkalic basalt. The proportion of the more enriched component is strongest where the ridge is shallowest, but it is clearly present to some extent everywhere. The Indian MORB-type mantle, in stations 31 and 32 (Fig. 1), marks the first appearance of the high $^{87}Sr/^{86}Sr$, ΔNd and $\Delta 8/4$Pb values (Fig. 4E–G) south of Heezen. Whatever its origin, Indian Ocean-like mantle was entrained along with the ascending Louisville plume mantle, and introduced to the vicinity of the Pacific–Antarctic risecrest at the same time.

To summarize, the ridge–hotspot interaction hypothesis claims that there are two general mantle types along the Pacific–Antarctic risecrest. One type is represented by depleted abyssal tholeiites comparable to those found elsewhere along the EPR, the other by an array of related compositions ranging from comparatively depleted tholeiites, with similarities to Indian Ocean type-MORB, and enriched basalts having in the extreme a Louisville plume-like signature. All of these may be derived from mantle materials added to this region, whether in dispersed or concentrated form, by advection associated with the plume. The strongly depleted mantle northeast of Heezen, which might be termed Pacific-type mantle, is fairly strongly influenced south of Heezen by both types of source peridotite along the risecrest for a distance of at least 300 km. This, and the shallow depths to the risecrest, are the immediate consequences of proximity of the Louisville hotspot to the PAR. In addition, the Indian MORB-type mantle is dynamically related to the Louisville plume in this region. The plume influence on the ridge, albeit subtle in geochemical terms, is nevertheless quite broad geographically. The plume itself may be geochemically zoned (cf. [52]), or it may have punched a deep layer of Indian MORB-type mantle upward into a depth range where it could begin to melt.

5.3. Large-scale magmatic segmentation

In the northerly EPR, MORB erupted along contiguous sections of the risecrest that have coherent isotopic and trace element compositions, such as those along the superfast spreading segments of the EPR at 13–23°S [37,38,52], have been proposed to define 'primary magmatic segments' [38,44]. Each segment is thought to contain magmas derived from a common, compositionally distinct mantle domain [53]. Our two hypotheses for the composition and dynamics of the upper mantle beneath the Pacific–Antarctic risecrest have different implications on the size of the mantle domain in the south Pacific. In the ridge–hotspot interaction hypothesis, the mantle source of the Pacific–Antarctic MORB is divided into a northeastern Pacific-type mantle source and a southwestern, heterogeneous, Louisville plume-influenced mantle source. The boundary of the two mantle domains is the Heezen transform of the Eltanin fault system, and is thus consistent with the proposal that these large mantle domains are bounded by the largest ridge tectonic offsets (e.g. [4,44]).

If there is a southwestward flow of the south Pacific asthenosphere, on the other hand, then the gradient in $^{143}Nd/^{144}Nd$ ratios, Na_8 and Ti_8 of N-MORB (Fig. 4A–C) indicates that the mantle from the Vacquier to Udintsev transforms belongs to a single mantle domain distributed over at least 1800 km beneath the Pacific–Antarctic risecrest. The observed continuity of mantle source composition across the Eltanin fault system also indicates that primary mantle domains are not necessarily bounded by the largest ridge tectonic offsets. Primary mantle domains reflect long (at least several hundred million years) time-integrated histories of these mantle sources to come up with detectable differences in radiogenic isotope ratios. On the other hand, the size of large ridge tectonic offsets such as transform faults are lithospheric tectonic features and grow

independently of the composition of the underlying mantle. These tectonic features grow in response to changing spreading rate and direction of the separating ridge axes, which in the case of the Eltanin fault system was only during the last 75 Ma (e.g. [16]). Hence, it is not required that the boundaries of primary mantle domains coincide with the largest ridge tectonic offsets. Of course, neither the mantle nor spreading ridges are stationary, at least with respect to one another, such that, in certain cases, boundaries of mantle geochemical zones and lithospheric tectonic boundaries unavoidably coincide. Hence, it is not surprising to observe that some of the boundaries of the primary magmatic segments in the northerly EPR coincide with large-offset transform faults (e.g. [44]).

6. Summary and conclusions

The variable isotopic and highly/moderately incompatible element ratios of Pacific–Antarctic risecrest and off-axis basalts indicate that the upper mantle there, like that beneath the northerly EPR and northeast Pacific ridges, is compositionally heterogeneous. We discern three isotopic end-members in the south Pacific upper mantle: (1) the 'depleted' type of material which is the source of Pacific N-MORB; (2) an 'enriched' source similar to that which produces basalts of the nearby Hollister Ridge; and (3) a source, restricted to two adjacent sample locations, similar to that of Indian MORB. As is generally true in the northerly Pacific, the source of the incompatible-element-depleted Pacific N-MORB is the upper mantle, which itself is variable in composition. The linear isotopic and trace element ratio arrays of N-MORB are a strong indication that the trends result from simple two-component mixing, with one end-member being depleted, the other by variably geochemically depleted to enriched sources which may occur as blobs, veinlets, or streaks within the depleted mantle domain. Mixing may occur in the mantle source prior to melting between solid materials, near the mantle source of the melts derived from these materials, or at crustal levels between magma batches or melt strains. The second end-member is that of an enriched source, the most extreme composition of which in this region is represented by lavas from the Louisville hotspot. In our study area, it is represented by alkalic basalts from the southeastern end of the Hollister Ridge. The third isotopic end-member is similar to that of Indian MORB-type mantle. The appearance of these two end-members in isolated samples along or close to the ridge axis suggests that their mantle sources are effectively isolated from the rest of the Pacific–Antarctic risecrest upper mantle, and thus their resultant lavas were able to survive the typical melting and mixing phenomena underneath the ridge axis.

The overall pattern of distribution of these heterogeneities along the Pacific–Antarctic risecrest leads us to propose two hypotheses to explain the nature and dynamics of the upper mantle in the south Pacific. One claims that the depleted N-MORB source forms a generally coherent reservoir, which displays a geochemical gradient with $^{143}Nd/^{144}Nd$ increasing and Na_8 and Ti_8 decreasing from northeast to southwest over 1800 km of ridges and intervening transform faults. This primary mantle domain is apparently unaffected by the presence of the large-offset transforms of the Eltanin system. The origin of the systematic northeast–southwest compositional gradient of the N-MORB mantle source beneath the ridges is not directly related to mixing between the depleted MORB sources and enriched Louisville plume; the gradient is only locally interrupted by the influence of the Louisville hotspot and the presence of Indian Ocean-type mantle. Instead, the geochemical gradient may be related to a proposal that the Pacific N-MORB mantle is flowing southwestward in response to the shrinking size of the Pacific basin, but the relationship is highly speculative at this time and needs further investigation.

The other hypothesis claims that there are two primary mantle domains beneath the Pacific–Antarctic risecrest. Northeast of the Heezen transform, of the Eltanin fault system, which is the most prominent and stable physical segment boundary in the Pacific, the mantle is similar to that elsewhere along the northern Pacific ridges, being mainly the depleted source of Pacific N-MORB. Southwest of the Heezen transform, the Pacific N-MORB mantle source is contaminated by Louisville mantle plume material, which also includes entrained Indian MORB-type mantle. The Louisville plume is pumped to the PAR through Hollister Ridge, represented by mildly alkalic lavas along its southern end.

Acknowledgements

Field and laboratory work was supported by National Science Foundation grants OCE93-00275 (Castillo), OCE94-11771 (Natland), OCE93-00352 (C.H. Langmuir for Niu), and OCE92-17707 (Lonsdale). We thank B. Hanan for assistance in Pb isotope analysis, J. Hawkins for critical review of an early version of the manuscript, and J. Mahoney, M. Perfit and an anonymous reviewer for helpful reviews. ***[FA]***

References

[1] C.H. Langmuir, J.F. Bender, R. Batiza, Petrologic and tectonic segmentation of the East Pacific Rise between 5°30′–14°30′N, Nature 222 (1986) 422–429.

[2] Y. Niu, R. Batiza, An empirical method for calculating melt compositions produced beneath mid-ocean ridges: application for axis and off-axis (seamounts) melting, J. Geophys. Res. 96 (1991) 21753–21777.

[3] J.M. Sinton, R.S. Detrick, Mid-ocean ridge magma chambers, J. Geophys. Res. 97 (1992) 197–216.

[4] K.C. Macdonald, P. Fox, L. Perram, M. Eisen, R. Haymon, S. Miller, S. Carbotte, M. Cormier, A. Shor, A new view of the mid-ocean ridge from the behavior of ridge axis discontinuities, Nature 335 (1988) 217–225.

[5] P. Lonsdale, Segmentation and disruption of the East Pacific Rise in the mouth of the Gulf of California, Mar. Geophys. Res. 17 (1995) 323–359.

[6] J.J. Mahoney, A.P. le Roex, Z. Peng, R.L. Fisher, J.H. Natland, Southwestern limits of Indian Ocean ridge mantle and the origin of low $^{206}Pb/^{204}Pb$ mid-ocean ridge basalt: isotope systematics of the central Southwest Indian Ridge (17°–50°E), J. Geophys. Res. 97 (1992) 19771–19790.

[7] D.G. Pyle, D.M. Christie, J.J. Mahoney, R.A. Duncan, Geochemistry and geochronology of ancient southeast Indian and southwest Pacific seafloor, J. Geophys. Res. 100 (1995) 22261–22282.

[8] P. Lonsdale, Geography of the southern (Pacific–Antarctic) East Pacific Rise and origin of its structural segmentation, J. Geophys. Res., 1994.

[9] P.R. Castillo, J.H. Natland, Y. Niu, Petrology and Sr, Nd and Pb isotope geochemistry of MORB from the fast-spreading ridges in the South Pacific, EOS Trans. Am. Geophys. Union 76 (1995) F530.

[10] P.R. Castillo, Y. Niu, J.H. Natland, S.H. Bloomer, P.F. Lonsdale, Trace element and isotopic investigation of the Pacific–Antarctic East Pacific Rise basalts; preliminary results, EOS Trans. Am. Geophys. Union 75 (1994) 742.

[11] J.H. Natland, Y. Niu, P.R. Castillo, P.F. Lonsdale, S.H. Bloomer, Petrologic exploration of the Pacific–Antarctic East Pacific Rise in the vicinity of the Udintsev and Eltanin transform faults, EOS Trans. Am. Geophys. Union 75 (1992) 742.

[12] C. DeMets, R.G. Gordon, D.F. Argus, S. Stein, Current plate motions, Geophys. J. Int. 101 (1990) 425–478.

[13] S.C. Cande, D.V. Kent, A new geomagnetic polarity time scale for the Late Cretaceous and Cenozoic, J. Geophys. Res. 97 (1992) 13917–13951.

[14] C.M. Weiland, K.C. Macdonald, Geophysical study of the East Pacific Rise 15°N–17°N: An unusually robust segment, J. Geophys. Res. 101 (1996) 20257–20273.

[15] SEIR Scientic Team, J.R. Cochran, J.-C. Sempere, The Southeast Indian Ridge between 88°E and 118°E: Gravity anomalies and crustal accretion at intermediate spreading rates, J. Geophys. Res. 102 (1997) 15463–15487.

[16] P. Lonsdale, Tectonic and magmatic ridges in the Eltanin fault system, South Pacific, Mar. Geophys. Res. 8 (1986) 203–242.

[17] K.C. Macdonald, Mid-Ocean ridges: Fine-scale tectonic, volcanic, and hydrothermal processes within the plate boundary zone, Annu. Rev. Earth Planet. Sci. 10 (1982) 155–190.

[18] J.-G. Schilling, R.H. Kingsley, J.D. Devine, Galapagos hot spot-spreading center system 1. Spatial Petrological and geochemical variations (83°W–101°W), J. Geophys. Res. 87 (1982) 5593–5610.

[19] J.A. Heirtzler, D.E. Hayes, E.M. Herron, W.C. Pittman, Preliminary report of volume 20 U.S.N.S. Eltanin Cruises 16-12, Lamont-Doherty Survey of the World Oceans, Tech. Rep. 3, 1969, 122 pp.

[20] W. Smith, D.T. Sandwell, Measured and estimated seafloor topography (version 4.2), World Data Center A for Marine Geology and Geophysics research publication RP-1, poster, 1997.

[21] D.S. Scheirer, K.C. Macdonald, D.W. Forsyth, S.P. Miller, D.J. Wright, M.-H. Cormier, C.H. Weiland, A map series of the southern East Pacific Rise and its flanks, 15°S to 19°S, Mar. Geophys. Res. 18 (1996) 1–12.

[22] D.T. Sandwell, E.L. Winterer, J. Mammerickx, R.A. Duncan, M.A. Lyych, D.A. Levitt, C.L. Johnson, Evidence for diffuse extension of the Pacific plate from Pukapuka ridges and cross-grain gravity lineations, J. Geophys. Res. 100 (1995) 15087–15099.

[23] W.F. Haxby, J.K. Weissel, Evidence for small-scale convention from Seasat altimeter data, J. Geophys. Res. 91 (1986) 3507–3520.

[24] A.E. Gripp, R.G. Gordon, Current plate velocities relative to the hotspots incorporating the NUVEL-1 plate motion model, Geophys. Res. Lett. 17 (1990) 1109–1112.

[25] C. Small, Observations of ridge–hotspot interactions in the Southern Ocean, J. Geophys. Res. 10 (1995) 17931–17946.

[26] P. Wessel, L. Kroenke, A geometric technique for relocating hotspots and refining absolute plate motions, Nature 387 (1997) 365–369.

[27] P. Lonsdale, Geography and history of the Louisville hotspot chain in the southwest Pacific, J. Geophys. Res. 93 (1988) 3078–3104.

[28] Q. Cheng, K.-H. Park, J.D. Macdougall, A. Zindler, G.W. Lugmair, H. Staudigel, J. Hawkins, P. Lonsdale, Isotopic

evidence for a hotspot origin of the Louisville Seamount Chain, in: B. Keating, P. Fryer, R. Batiza, G. Boehlert (Eds.), Seamounts, Islands and Atolls, Am. Geophys. Union Monogr. 43 (1987) 283–296.
[29] G. Thompson, W.B. Bryan, R. Ballard, K. Hamuro, W.G. Melson, Axial processes along a segment of the East Pacific Rise, 10°–12°N, Nature 318 (1985) 429–433.
[30] M.R. Perfit, D.J. Fornari, M.C. Smith, J.F. Bender, C.H. Langmuir, R.M. Haymon, Small-scale spatial and temporal variations in mid-ocean ridge crest magmatic processes, Geology 22 (1994) 375–379.
[31] R. Batiza, D. Vanko, Petrology of young Pacific seamounts, J. Geophys. Res. 89 (1984) 11235–11260.
[32] J.H. Natland, Partial melting of a lithologically heterogeneous mantle: inferences from crystallization histories of magnesian abyssal tholeiites from the Siquieros Fracture Zone, in: A.D. Saunders, M.J. Norry (Eds.), Magmatism in the Ocean Basins, Geol. Soc. London Spec. Publ. 42 (1989) 41–70.
[33] R. Hekinian, D. Bideau, R. Hebert, Y. Niu, Magmatism in the Garret transform fault (East Pacific Rise near 13°27′S), J. Geophys. Res. 100 (1995) 10163–10185.
[34] M.R. Perfit, D.J. Fornari, W.I. Ridley, P.D. Kirk, J. Casey, K.A. Kastens, J.R. Reynolds, M. Edwards, D. Desonie, R. Shuster, S. Paradis, Recent volcanism in the Siquieros transform fault: picritic basalts and implications for MORB magma genesis, Earth Planet. Sci. Lett. 14 (1996) 91–108.
[35] P.E. Janney, P.R. Castillo, Geochemistry of Mesozoic Pacific MORB: Constraints on melt generation and the evolution of the Pacific upper mantle, J. Geophys. Res. 102 (1997) 5207–5229.
[36] I. Vlastelic, L. Dosso, J. Etoubleau, J.-L. Joron, H. Bougault, L. Geli, PACANTARCTIC Sci. Party, New geochemical data from the Pacific–Antarctic Ridge and the Hollister Ridge, Terra Nova 9 Abstr. Suppl. #1 (1997) 515.
[37] J.J. Mahoney, J.M. Sinton, M.D. Kurz, J.D. Macdougall, K.J. Spencer, G.W. Lugmair, Isotope and trace element characteristics of a super-fast spreading ridge: East Pacific Rise, 13–23°S, Earth Planet Sci. Lett. 121 (1994) 173–193.
[38] W. Bach, E. Hegner, J. Erzinger, M. Satir, Chemical and isotopic variations along the superfast spreading East Pacific Rise from 6 to 30°S, Contrib. Mineral. Petrol. 116 (1994) 365–380.
[39] S.R. Hart, D.C. Gerlach, W.M. White, A possible new Sr–Nd–Pb mantle array and consequences for mantle mixing, Geochim. Cosmochim. Acta 50 (1986) 1551–1557.
[40] S.R. Hart, Heterogeneous mantle domains, genesis and mixing chronologies, Earth Planet. Sci. Lett. 90 (1988) 273–296.
[41] W.M. White, A. Hofmann, H. Puchelt, Isotope geochemistry of Pacific mid-ocean ridge basalt, J. Geophys. Res. 92 (1987) 4881–4893.
[42] Y. Niu, D.G. Waggoner, J.M. Sinton, J.J. Mahoney, Mantle source heterogeneity and melting processes in the Hump region: East Pacific Rise 18°–19°S, J. Geophys. Res. 101 (1996) 27711–27733.
[43] B. Hamelin, B. Dupre, C. Allegre, Lead–strontium isotopic variations along the East Pacific Rise and the Mid-Atlantic Ridge: a comparative study, Earth Planet. Sci. Lett. 67 (1984) 340–350.
[44] J.M. Sinton, S.M. Smaglik, J.J. Mahoney, Magmatic processes at superfast spreading mid-ocean ridges: glass compositional variations along the East Pacific Rise 13–23°S, J. Geophys. Res. 96 (1991) 6133–6155.
[45] R. Lanyon, A.J. Crawford, S.M. Eggins, Westward migration of Pacific Ocean upper mantle into the Southern Ocean region between Australia and Antarctica, Geology 23 (1995) 511–514.
[46] W. Alvarez, Geologic evidence for the plate driving mechanism: The continental undertow hypothesis and the Australian–Antarctic Discordance, Tectonics 9 (1990) 1213–1220.
[47] K.M. Marks, J.M. Stock, Variations in ridge morphology and depth–age relationships on the Pacific–Antarctic Ridge, J. Geophys. Res. 99 (1994) 531–541.
[48] M. Sahabi, L. Geli, J.-L. Olivet, L. Gilg-Capar, G. Roult, H. Ondreas, P. Beuzart, D. Aslanian, Morphological reorganization within the Pacific–Antarctic Discordance, Earth Planet. Sci. Lett. 137 (1996) 157–173.
[49] E.M. Klein, J. Karsten, Ocean ridge basalts with convergent margin geochemical affinities from the southern Chile Ridge, Nature 374 (1995) 52–57.
[50] P.R. Castillo, The Dupal anomaly as a trace of the upwelling lower mantle, Nature 336 (1988) 667–670.
[51] B.B. Hanan, J.-G. Schilling, Easter microplate evolution: Pb isotope evidence, J. Geophys. Res. 94 (1989) 7432–7448.
[52] R.A. Duncan, M.A. Richards, Hotspots, mantle plumes, flood basalts, and true polar wander, Rev. Geophys. 29 (1991) 31–50.
[53] R. Batiza, Magmatic segmentation of mid-ocean ridges: a review, in: C.J. Macleod, P. Taylor, C.L. Walker (Ed.), Tectonic, Magmatic, Hydrothermal and Biological Segmentation of Mid-Ocean Ridges, Geol. Soc. London Spec. Publ. 118 (1996) 103–130.
[54] W. Todt, R.A. Cliff, A. Hanser, A.W. Hofmann, $^{202}Pb + ^{205}Pb$ double spike for lead isotopic analysis, Terra Cognita 4 (1984) 209.
[55] N.M. Evensen, P.J. Hamilton, R.K. O'Nions, Rare earth element abundances in chondritic meteorites, Geochim. Cosmochim. Acta 42 (1987) 145–152.